A Structural Comparison of Two Thallium Copper Erbium Sulfides: $TlCu_3Er_2S_5$ and $Tl_2Cu_5Er_3S_8$

Marcel A. Eberle[a], Jean-Marie Babo[b] and Thomas Schleid[a]

[a] University of Stuttgart, Institute for Inorganic Chemistry, Pfaffenwaldring 55, D-70569 Stuttgart, Germany

[b] Department of Civil Engineering and Geological Sciences and Department of Chemistry and Biochemistry, University of Notre Dame, Notre Dame, IN 46556, USA

Reprint requests to Prof. Dr. Th. Schleid. E-mail: schleid@iac.uni-stuttgart.de

Z. Naturforsch. **2014**, *69b*, 851 – 858 / DOI: 10.5560/ZNB.2014-4074
Received April 8, 2014

Orange $TlCu_3Er_2S_5$ crystallizes in the orthorhombic space group *Cmcm* ($a = 391.27(2)$, $b = 1382.91(7)$, $c = 1630.54(8)$ pm, $Z = 4$). Its crystal structure contains one Tl^+, one Er^{3+}, two Cu^+, and three S^{2-} ions as crystallographically unique components. All Cu^+ cations are coordinated by four S^{2-} anions to form $[CuS_4]^{7-}$ tetrahedra, which have vertex- and edge-connectivity to build up $^2_\infty\{[Cu_3S_5]^{7-}\}$ layers parallel to the (010) plane. The Er^{3+} cations are octahedrally surrounded by six S^{2-} anions. These $[ErS_6]^{9-}$ units share *trans*-oriented edges forming linear chains, which are further linked by common vertices yielding $^1_\infty\{[Er_2S_{10}]^{14-}\}$ double strands. Further fusion *via* common vertices results in $^2_\infty\{[Er_2S_5]^{4-}\}$ layers parallel to the (010) plane. Alternatingly stacked along [010] and condensed *via* S^{2-} anions, these two types of layers form a three-dimensional framework, leaving tunnels along [100], where the Tl^+ cations fit in. These are each coordinated by eight S^{2-} anions in the shape of bicapped trigonal prisms. $Tl_2Cu_5Er_3S_8$ was obtained as black single crystals with metallic luster (monoclinic, *Cm*, $a = 1381.69(7)$, $b = 390.73(2)$, $c = 1435.98(7)$ pm, $\beta = 111.132(3)^\circ$, $Z = 2$). Four of the five crystallographically different Cu^+ cations are tetrahedrally surrounded by S^{2-} anions, whereas $(Cu3)^+$ is situated in sulfur triangles. Connected *via* common vertices and edges, the copper-sulfur polyhedra form strongly corrugated $^2_\infty\{[Cu_5S_8]^{11-}\}$ layers parallel to the $(20\bar{1})$ plane. All Er^{3+} cations are again coordinated by six S^{2-} anions in the shape of $[ErS_6]^{9-}$ octahedra. Their condensation *via* edges and vertices leads to $^2_\infty\{[Er_3S_8]^{7-}\}$ layers spreading out parallel to the (010) plane. Both types of anionic layers result in a three-dimensional framework through sulfide fusion, which leaves tunnels running along [010] occupied by Tl^+ cations. The two crystallographically different Tl^+ cations both have eight coordinating S^{2-} anions forming bicapped trigonal prisms. Remarkably enough, the ion closest to $(Tl1)^+$ is not a S^{2-} anion (shortest Tl^+–S^{2-} bond: 305 pm), but a $(Cu3)^+$ cation at a distance of just 291 pm.

Key words: Thallium, Copper, Erbium, Sulfides, Solid-State Crystal Structures

Introduction

Quaternary compounds containing a trivalent rare-earth metal, a monovalent alkali metal along with monovalent copper and a chalcogen as anionic component have been observed with several different compositions and crystal structures, which very often have common structural features. Typically, three-dimensional frameworks of condensed rare-earth metal-centered chalcogenide octahedra are built, leaving tunnels, in which all monovalent cations fit in. As examples serve the sulfides $KCuM_2S_4$ (M = Y; Nd, Sm, Gd, Tb, Ho) [1, 2], where $[MS_6]^{9-}$ octahedra (CN = 6) form a three-dimensional framework with tunnels along [100], in which Cu^+ and K^+ cations are found surrounded by four and eight S^{2-} anions, respectively, as polyhedra with the shape of tetrahedra (CN = 4) or bicapped trigonal prisms (CN = 8). Within the crystal structure of the compounds $RbCu_3M_2S_5$ (M = Ho, Er) [3, 4] as well as the isotypically crystallizing representatives $CsCu_3M_2S_5$ (M = Dy, Er) [5], the three-dimensional framework is not only made up of $[MS_6]^{9-}$ octahedra, but also of $[CuS_4]^{7-}$ tetrahedra. The remaining tunnels are again filled with the monovalent cations (Rb^+ or Cs^+), which have eight neighboring S^{2-} anions forming bi-

capped trigonal prisms. Considering Tl^+ as a monovalent pseudo-alkali metal cation in analogous systems, it is possible to maintain the same structure types that are already known with the heavy alkali metals. In fact, this is the case for $KCuGd_2S_4$-type [2] $TlCuY_2S_4$ [6], and $TlCu_3Lu_2Se_5$ [7], crystallizing isotypically with the $RbCu_3M_2S_5$ (M = Ho, Er) [3, 4] and $CsCu_3M_2S_5$ (M = Dy, Er) [5] series. In some other compounds, however, new structural features appear caused by the lone-pair electrons at the Tl^+ cations. In combination with a coinage metal like gold, the cation pair $[Tl^+Au^+]$ is isoelectronic with the well known $[Hg_2]^{2+}$ dumbbell [8]. Moreover, $[Tl^+Ag^+]$ and $[Tl^+Cu^+]$ units can therefore be considered as pseudo-isoelectronic as discussed in [9]. Such attractive cation-cation interactions are indeed found in $Tl_3Ag_3Sb_2S_6$ [9], where the closest $Tl^+\cdots Ag^+$ contacts are 296 pm and therefore shorter than the common Tl^+–S^{2-} bonds (299 – 367 pm) in this compound. No such interactions are seen in $TlCu_3Er_2S_5$, but in $Tl_2Cu_5Er_3S_8$, where the closest $Tl^+\cdots Cu^+$ contact (291 pm) is also smaller than the shortest Tl^+–S^{2-} distance (305 pm).

Experimental Section

Preparation

Orange $TlCu_3Er_2S_5$ was obtained by the reaction of a mixture of Cu (99.9 %, Sigma-Aldrich, St. Louis, MO, USA), Er and S (both 99.9 %, ChemPur, Karlsruhe, Germany) in a molar ratio of 2 : 1 : 3, along with an excess of TlCl (99.9 %, Merck, Darmstadt, Germany) as flux and thallium source. Black $Tl_2Cu_5Er_3S_8$ emerged from a mixture of

Table 1. Crystal structure data for $TlCu_3Er_2S_5$ (left) and $Tl_2Cu_5Er_3S_8$ (right).

Compound	$TlCu_3Er_2S_5$	$Tl_2Cu_5Er_3S_8$
Crystal system	orthorhombic	monoclinic
Space group	*Cmcm* (no. 63)	*Cm* (no. 8)
a, pm	391.27(2)	1381.69(7)
b, pm	1382.91(7)	390.73(2)
c, pm	1630.54(8)	1435.98(7)
β, deg	90	111.132(3)
Z	4	2
D_x, g cm^{-3}	6.70	6.82
Absorption coefficient μ, mm^{-1}	45.2	47.7
$F(000)$, e$^-$	1536	1278
Index range hkl	±5, ±18, ±21	±18, ±5, ±19
$2\theta_{max}$, deg	55.7	56.8
Reflections measured/unique	6123/619	9576/1983
Parameters refined	38	111
R_{int}/R_σ	0.084/0.038	0.075/0.052
R_1 for n observed reflections with $\lvert F_o\rvert > 4\,\sigma(F_o)$	0.026	0.032
Number (n) of observed reflections	569	1817
R_1/wR_2 for all reflections	0.030/0.059	0.038/0.062
x Flack	–	0.35(13)[a]
GooF	1.076	1.043
Extinction coefficient (g)	0.00261(13)	0.00083(5)
Residual electron density, $\rho_{min./max.}$, e$^- \times 10^{-6}$ pm^{-3}	1.76/−2.03	1.35/−1.73

[a] Thus refined as inversion twin.

Table 2. Atomic coordinates for $TlCu_3Er_2S_5$ [a] and $Tl_2Cu_5Er_3S_8$ [b].

	Wyckoff site		x/a		y/b		z/c	
	[a]	[b]	[a]	[b]	[a]	[b]	[a]	[b]
Tl1	4*c*	2*a*	0	0[a]	0.92888(4)	0	1/4	0[a]
Tl2	–	2*a*	–	0.62849(6)	–	0	–	0.41366(6)
Cu1	4*c*	2*a*	0	0.2831(2)	0.64639(14)	0	1/4	0.0178(2)
Cu2	8*f*	2*a*	0	0.3427(2)	0.41795(9)	0	0.04146(9)	0.4072(2)
Cu3	–	2*a*	–	0.0216(2)	–	0	–	0.2094(2)
Cu4	–	2*a*	–	0.2129(2)	–	0	–	0.6624(2)
Cu5	–	2*a*	–	0.4141(2)	–	0	–	0.7577(2)
Er1	8*f*	2*a*	0	0.96297(6)	0.19145(3)	0	0.40582(2)	0.59242(6)
Er2	–	2*a*	–	0.66647(6)	–	0	–	0.82781(6)
Er3	–	2*a*	–	0.80256(6)	–	0	–	0.21243(6)
S1	4*c*	2*a*	0	0.4246(4)	0.2425(2)	0	1/4	0.1694(4)
S2	8*f*	2*a*	0	0.6854(4)	0.43776(15)	0	0.61570(15)	0.0163(4)
S3	8*f*	2*a*	0	0.3053(4)	0.17039(15)	0	0.57023(15)	0.8505(4)
S4	–	2*a*	–	0.1951(4)	–	0	–	0.2583(4)
S5	–	2*a*	–	0.9402(4)	–	0	–	0.4016(4)
S6	–	2*a*	–	0.3241(4)	–	0	–	0.5701(4)
S7	–	2*a*	–	0.6125(4)	–	0	–	0.6262(4)
S8	–	2*a*	–	0.0158(4)	–	0	–	0.7933(4)

[a] Arbitrarily fixed for a proper definition of the origin.

the same reactands in a molar ratio of 5 : 3 : 8, but also with an excess of TlCl as reactive flux. Both reactions took place in evacuated silica ampoules within eight days at 850 °C. The single crystals of $TlCu_3Er_2S_5$ are transparent with glassy luster, whereas those of $Tl_2Cu_5Er_3S_8$ exhibit a metallic glint. Both reaction products could be washed with hot water to remove thallium chloride-containing by-products, because of the water- and air-stability of the coarse single crystals.

X-Ray structure determination

Intensity data sets for the single crystals of $TlCu_3Er_2S_5$ and $Tl_2Cu_5Er_3S_8$ were collected with a Nonius Kappa-CCD diffractometer using graphite-monochromatized Mo K_α radiation (wavelength: $\lambda = 71.07$ pm). Numerical absorption corrections were performed with the help of the program HABITUS [10]. The structure solutions and refinements were carried out by using the program package SHELX-97 [11]. Details of the data collections and the structure refinements [12] are summarized in Table 1. Atomic positions and coefficients of the equivalent isotropic displacement parameters [13] can be found in Tables 2 and 3. Selected interatomic distances are listed in Table 4, while Table 5 displays the motifs of mutual adjunction [14] for both crystal structures.

Further details of the crystal structure investigations may be obtained from Fachinformationszentrum Karlsruhe, 76344 Eggenstein-Leopoldshafen, Germany (fax: +49-7247-808-666; e-mail: crysdata@fiz-karlsruhe.de, http://www.fiz-karlsruhe.de/request_for_deposited_data.html) on quoting the deposition numbers CSD-423716 for $TlCu_3Er_2S_5$ and CSD-427358 for $Tl_2Cu_5Er_3S_8$.

Table 3. Anisotropic displacement parameters for $TlCu_3Er_2S_5$ (top) and $Tl_2Cu_5Er_3S_8$ (bottom).

$TlCu_3Er_2S_5$	U_{11}	U_{22}	U_{33}	U_{23}	U_{eq} [a]
Tl	254(4)	230(3)	231(4)	0	238(2)
Cu1	163(10)	274(10)	178(10)	0	205(4)
Cu2	155(7)	121(6)	338(8)	−39(5)	205(3)
Er	69(3)	71(2)	70(3)	−2(1)	70(2)
S1	122(16)	111(14)	42(14)	0	92(6)
S2	90(11)	49(9)	119(11)	23(8)	86(5)
S3	68(11)	60(9)	79(10)	5(8)	69(4)

[a] $U_{eq} = 1/3\ (U_{11} + U_{22} + U_{33})$; $U_{13} = U_{12} = 0$ for all atoms.

$Tl_2Cu_5Er_3S_8$	U_{11}	U_{22}	U_{33}	U_{13}	U_{eq} [a]
Tl1	270(5)	255(6)	197(6)	112(4)	233(3)
Tl2	277(5)	198(6)	199(6)	116(4)	216(3)
Cu1	207(14)	146(17)	154(17)	−17(12)	192(7)
Cu2	208(13)	153(17)	181(17)	57(12)	184(7)
Cu3	106(12)	161(16)	357(21)	61(11)	214(8)
Cu4	166(14)	142(18)	270(19)	117(13)	183(7)
Cu5	157(13)	150(18)	269(19)	118(13)	180(7)
Er1	77(4)	57(5)	70(5)	24(4)	69(2)
Er2	79(4)	60(5)	52(5)	21(4)	64(2)
Er3	77(4)	69(5)	64(5)	22(4)	71(2)
S1	53(20)	79(28)	62(23)	13(18)	66(11)
S2	131(24)	44(30)	122(30)	91(22)	92(11)
S3	94(22)	48(28)	141(32)	80(22)	87(11)
S4	67(21)	100(29)	113(28)	61(20)	86(11)
S5	94(23)	101(31)	43(25)	−7(19)	88(11)
S6	60(20)	103(30)	77(28)	9(20)	84(11)
S7	86(21)	39(28)	143(32)	74(21)	83(11)
S8	66(20)	60(28)	58(27)	27(19)	61(11)

[a] $U_{eq} = 1/3\ [U_{22} + 1/\sin^2\beta\ (U_{11} + U_{33} + 2U_{13}\cos\beta)]$; $U_{12} = U_{23} = 0$ for all atoms.

Table 4. Selected interatomic distances (in pm) for $TlCu_3Er_2S_5$ (left) and $Tl_2Cu_5Er_3S_8$ (right).

	$TlCu_3Er_2S_5$			$Tl_2Cu_5Er_3S_8$		
Tl1	– S1	323.6	(2 ×)	– S8	305.4	(1 ×)
	– S3	323.7	(2 ×)	– S2	316.2	(2 ×)
	– S2	346.8	(4 ×)	– S3	339.1	(2 ×)
	– *S1′*	*433.7*	(1 ×)	– S1	355.6	(2 ×)
	··· *Cu1*	*358.8*	(1 ×)	– S4	371.7	(2 ×)
				··· *Cu3*	*291.3*	(1 ×)
Tl2				– S7	313.8	(1 ×)
				– S5	320.8	(2 ×)
				– S4	333.5	(2 ×)
				– S6	343.4	(2 ×)
				– S1	362.1	(1 ×)
				··· *Cu3*	*338.8*	(2 ×)
Cu1	– S1	236.5	(2 ×)	– S1	234.4	(1 ×)
	– S2	248.0	(2 ×)	– S2	237.0	(2 ×)
				– S3	252.9	(1 ×)
Cu2	– S2	233.4	(1 ×)	– S4	236.4	(1 ×)
	– S3	235.4	(2 ×)	– S5	239.1	(2 ×)
	– S2′	257.7	(1 ×)	– S6	244.4	(1 ×)
	··· *Cu2′*	*264.2*	(1 ×)			
Cu3				– S4	224.2	(1 ×)
				– S1	232.1	(2 ×)
				··· *Tl1*	*291.3*	(1 ×)
				··· *Tl2*	*338.8*	(2 ×)
Cu4				– S7	234.3	(2 ×)
				– S6	236.3	(1 ×)
				– S3	253.8	(1 ×)
				··· *Cu5*	*261.9*	(1 ×)
Cu5				– S3	234.1	(1 ×)
				– S8	235.3	(2 ×)
				– S6	252.7	(1 ×)
				··· *Cu4*	*261.9*	(1 ×)
Er1	– S1	263.7	(1 ×)	– S5	264.3	(1 ×)
	– S2	267.3	(2 ×)	– S6	267.5	(2 ×)
	– S3	269.7	(1 ×)	– S8	270.8	(1 ×)
	– S3′	276.2	(2 ×)	– S7	275.6	(2 ×)
Er2				– S2	262.4	(1 ×)
				– S3	267.4	(2 ×)
				– S7	271.7	(1 ×)
				– S8	276.6	(2 ×)
Er3				– S4	267.6	(2 ×)
				– S2	269.5	(1 ×)
				– S5	269.6	(1 ×)
				– S1	279.2	(2 ×)

Table 5. Motifs of mutual adjunction [14] for $TlCu_3Er_2S_5$ (top) and $Tl_2Cu_5Er_3S_8$ (bottom).

$TlCu_3Er_2S_5$	S1	S2	S3	CN
Tl	2/2	4/2	2/1	8
Cu1	2/2	2/1	0/0	4
Cu2	0/0	2/2	2/2	4
Er	1/2	2/2	3/3	6
CN	6	7	6	

$Tl_2Cu_5Er_3S_8$	S1	S2	S3	S4	S5	S6	S7	S8	CN
Tl1	2/2	2/2	2/2	1/1	0/0	0/0	0/0	1/1	8
Tl2	1/1	0/0	0/0	2/2	2/2	2/2	1/1	0/0	8
Cu1	1/1	2/2	1/1	0/0	0/0	0/0	0/0	0/0	4
Cu2	0/0	0/0	0/0	1/1	2/2	1/1	0/0	0/0	4
Cu3	2/2	0/0	0/0	1/1	0/0	0/0	0/0	0/0	3
Cu4	0/0	0/0	1/1	0/0	0/0	1/1	2/2	0/0	4
Cu5	0/0	0/0	1/1	0/0	0/0	1/1	0/0	2/2	4
Er1	0/0	0/0	0/0	0/0	1/1	2/2	2/2	1/1	6
Er2	0/0	1/1	2/2	0/0	0/0	0/0	1/1	2/2	6
Er3	2/2	1/1	0/0	2/2	1/1	0/0	0/0	0/0	6
CN	8	6	7	7	6	7	6	6	

Results

Structure description of $TlCu_3Er_2S_5$

The needle-shaped orange single crystals of $TlCu_3Er_2S_5$ turned out to crystallize isotypically with those of the whole $TlCu_3M_2S_5$ series (M = Sc; Tm – Lu) [15] (orthorhombic, *Cmcm*; for details see Table 1) with the $CsCu_3Er_2S_5$-type structure [5]. The two crystallographically different Cu^+ cations are each coordinated by four S^{2-} anions forming distorted tetrahedra ($d(Cu^+–S^{2-})$ = 233 – 258 pm). While the angles within these $[CuS_4]^{7-}$ tetrahedra around $(Cu1)^+$ differ quite a lot ($\angle$(S–Cu1–S) = 105 – 124°), those within the sulfur tetrahedra centered by $(Cu2)^+$ are more similar to each other ($\angle$(S–Cu2–S) = 105 – 115°). Interconnection of the $[CuS_4]^{7-}$ tetrahedra results in single $^1_\infty\{[(Cu1)S^t_{2/1}S^v_{2/2}]^{4-}\}$ chains with just two connections per tetrahedron *via* vertices, as well as in $^1_\infty\{[(Cu2)S^e_{2/2}S^v_{2/2}]^{3-}\}$ strands with connections *via* one edge and two vertices (Fig. 1, top and mid). Both features are found fused by common vertices to form corrugated $^2_\infty\{[Cu_3S_5]^{7-}\}$ layers, which spread out parallel to the (010) plane. The crystallographically unique Er^{3+} cations are surrounded by six S^{2-} anions in the shape of fairly regular $[ErS_6]^{9-}$ octahedra ($d(Er^{3+}–S^{2-})$ = 264 – 276 pm, $\angle$(S–Er–S) = 86 – 94°, 171 – 189°). These $[ErS_6]^{9-}$ units are connected *via* common edges to form $^1_\infty\{[Er_2S_{10}]^{14-}\}$ double chains along the [100] direction (Fig. 2). Linked by common vertices, these chains result in $^2_\infty\{[Er_2S_5]^{4-}\}$ slabs within the (010) plane, which therefore run parallel to the above-mentioned $^2_\infty\{[Cu_3S_5]^{7-}\}$ layers. These two different types of anionic sheets are alternatingly stacked and condensed building up a three-dimensional $^3_\infty\{[Cu_3Er_2S_5]^-\}$ framework (Fig. 3) with tunnels propagating along [100]. The tunnel-like cavities formed this way become finally occupied with the monovalent Tl^+ cations. Surrounded by eight S^{2-} anions ($d(Tl^+–S^{2-})$ = 324 – 347 pm), the coordination polyhedra around Tl^+ are best described as bicapped trigonal prisms (Fig. 4). A possible third cap exists in the crystal structure of $TlCu_3Er_2S_5$, but the distance of 434 pm from the capping S^{2-} anion (S1′) to the central Tl^+ cation is much larger than all the other $Tl^+–S^{2-}$ bond lengths (see Table 4).

Structure description of $Tl_2Cu_5Er_3S_8$

Black $Tl_2Cu_5Er_3S_8$ crystallizes monoclinically (*Cm*, Z = 2; for details see Table 1) and contains eighteen crystallographically different ions (two Tl^+, five Cu^+, three Er^{3+} and eight S^{2-}) all occupying Wyckoff positions 2*a*. Whereas the $(Cu1)^+$ and $(Cu2)^+$ cations form single chains of vertex-connected tetrahedra with the composition $^1_\infty\{[CuS^v_{2/2}S^t_{2/1}]^{5-}\}$ (Fig. 1, top), the $(Cu4)^+$ and $(Cu5)^+$ cations build up $^1_\infty\{[CuS^e_{2/2}S^v_{2/2}]^{3-}\}$ strands of vertex-sharing congonial bitetrahedra $[Cu_2S_6]^{10-}$ (Fig. 1, mid), which consist of two edge-connected $[CuS_4]^{7-}$ units. Bond lengths ($d(Cu^+–S^{2-})$ = 234 – 254 pm) as well as bond angles ($\angle$(S–Cu–S) = 105 – 122°) indicate rather distorted tetrahedra. In contrast to the aforementioned Cu^+ cations, $(Cu3)^+$ has only three adjoining S^{2-} anions. This results in vertex-connected $[(Cu3)S_3]^{5-}$ triangles (Fig. 5, $d((Cu3)^+–S^{2-})$ = 224 – 232 pm) that evolve into linear $^1_\infty\{[(Cu3)S^t_{1/1}S^v_{2/2}]^{3-}\}$ chains running along the *b* axis (Fig. 1, bottom). The connection of all described copper-bearing sulfide chains yields strongly corrugated $^2_\infty\{[Cu_5S_8]^{11-}\}$ layers parallel to the $(20\bar{1})$ plane. The Er^{3+} cations are again coordinated by six S^{2-} anions in the shape of octahedra with bond lengths from 262 up to 279 pm (see Table 4), and S–Er–S angles within the intervals 85 – 95° and 170 – 190°. The $[(Er1)S_6]^{9-}$ and $[(Er2)S_6]^{9-}$ octahedra share common edges and build up $^1_\infty\{[Er_2S_{10}]^{14-}\}$ double chains along the [010] direction. Besides this structural motif, which can also be seen in the crystal structure of $TlCu_3Er_2S_5$, $[(Er3)S_6]^{9-}$ octahedra first form $^1_\infty\{[(Er3)S^t_{2/1}S^e_{4/2}]^{5-}\}$

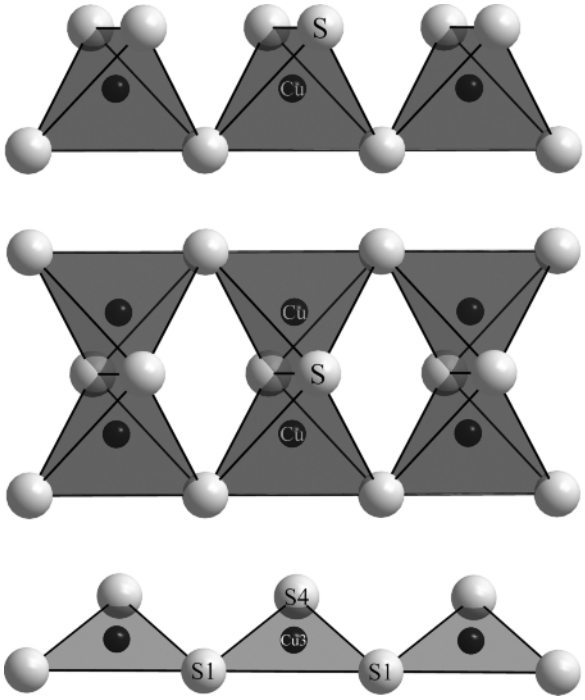

Fig. 1. Connection of polyhedra made up by S^{2-} anions surrounding Cu^+ cations in the crystal structures of $TlCu_3Er_2S_5$ (top and mid) and $Tl_2Cu_5Er_3S_8$ (top, mid and bottom).

single chains just by sharing the *trans*-oriented edges. These two types of erbium-bearing sulfide chains are alternatingly stacked and condensed by common vertices to form $^2_\infty\{[Er_3S_8]^{7-}\}$ layers parallel to the (010) plane (Fig. 5). Both kinds of anionic slabs $^2_\infty\{[Cu_5S_8]^{11-}\}$ and $^2_\infty\{[Er_3S_8]^{7-}\}$ together form

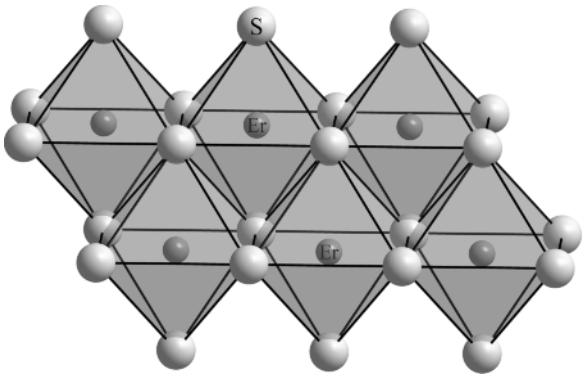

Fig. 2. View at the double chains built up by fused $[ErS_6]^{9-}$ octahedra in $TlCu_3Er_2S_5$.

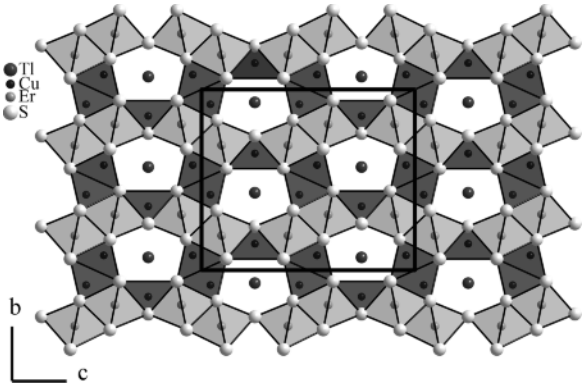

Fig. 3. The three-dimensional framework in the crystal structure of $TlCu_3Er_2S_5$.

a three-dimensional $^3_\infty\{[Cu_5Er_3S_8]^{2-}\}$ framework by sulfide fusion (Fig. 6) with channels occupied by the monovalent Tl^+ cations. Both crystallographically unique Tl^+ cations are coordinated by eight S^{2-} anions in bicapped trigonal prisms (Fig. 7). Condensed *via* common faces, the bicapped trigonal prisms form linear $^1_\infty\{[TlS^t_{2/1}S^f_{6/2}]^{9-}\}$ chains along [010]. Two of these adjacent chains share S^{2-} anions in a way that one cap of a bicapped trigonal prism represents a vertex of the opposite one and *vice versa* yielding $^1_\infty\{([TlS^t_{1/1}S^f_{4/2}S^{f/c}_{3/2}]^{8-})_2\}$ double strands. Each double strand has a gap in between the chains of face-connected prisms, in which a $^1_\infty\{[(Cu3)S^t_{1/1}S^v_{2/2}]^{3-}\}$ chain of vertex-sharing $[(Cu3)S_3]^{5-}$ triangles fits in. Therefore, $(Cu3)^+$ and Tl^+ cations are getting quite

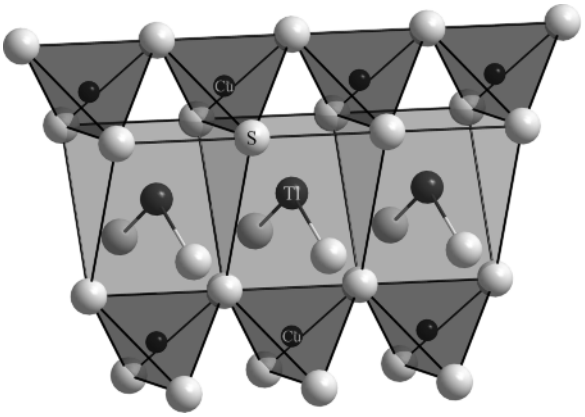

Fig. 4. Chains of vertex-shared $[CuS_4]^{7-}$ tetrahedra attached to strands of trigonal prisms surrounding the Tl^+ cations in the crystal structures of $TlCu_3Er_2S_5$ and $Tl_2Cu_5Er_3S_8$.

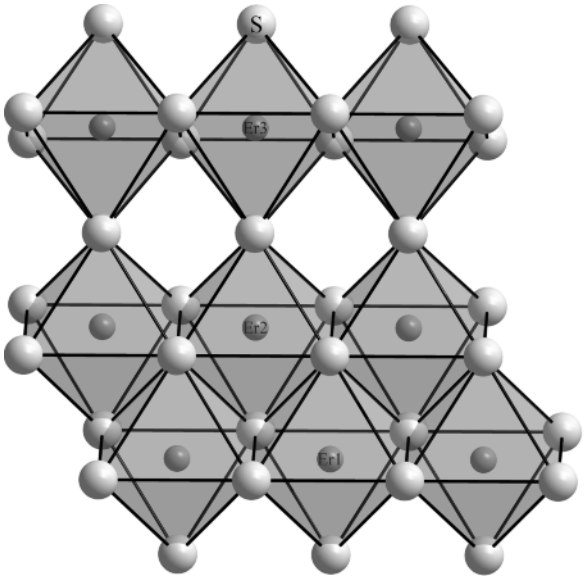

Fig. 5. Interconnection of the $[ErS_6]^{9-}$ octahedra in $Tl_2Cu_5Er_3S_8$.

close to each other (Fig. 7). While the $(Tl2)^+\cdots(Cu3)^+$ distance with a length of 339 pm (2 ×) is roughly as long as the average $(Tl2)^+$–S^{2-} bond ($\langle d \rangle = 334$ pm), the unique $(Tl1)^+\cdots(Cu3)^+$ distance has just a length of 291 pm. This value is even smaller than the shortest Tl^+–S^{2-} distance (305 pm) in the whole compound,

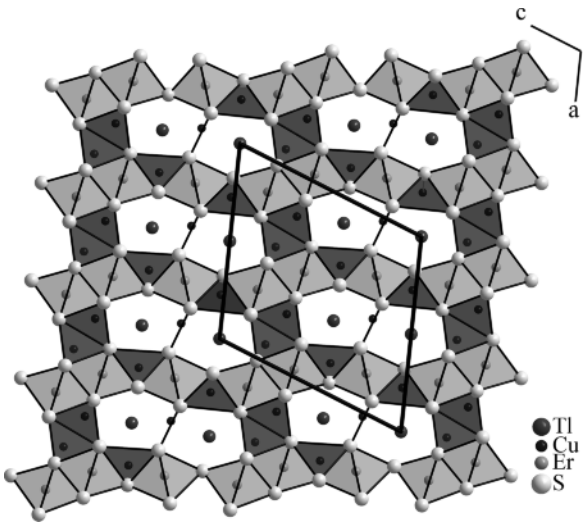

Fig. 6. The three-dimensional framework in the crystal structure of $Tl_2Cu_5Er_3S_8$.

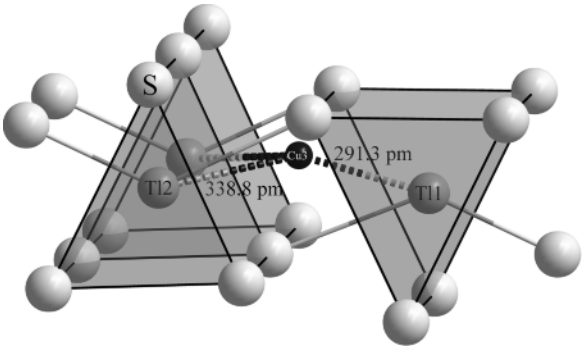

Fig. 7. Shortest $Tl^+\cdots Cu^+$ contacts (Tl1···Cu3, 1 ×; Tl2···Cu3, 2 ×) in the crystal structure of $Tl_2Cu_5Er_3S_8$.

giving evidence for possible attractive interactions between these two sorts of cations.

Discussion and Conclusion

The two title compounds show that Tl^+ cations can act in different ways in solid-state crystal structures. In the crystal structure of $TlCu_3Er_2S_5$ they can be regarded as normal $6s^2$ balls, spherical like alkali-metal cations, which is not very astonishing as their cationic crystal radius (173 pm for CN = 8) [16] is just slightly smaller than that of Rb^+ (175 pm for CN = 8) [16]. The isotypic sulfides $ACu_3Er_2S_5$ with A = Tl, Rb [4] or Cs [5] illustrate this fact clearly. They all crystallize orthorhombically in space group *Cmcm* with four formula units per unit cell. An increase of the cationic radius of the A^+ cation leads to an increase of the lattice parameters ($TlCu_3Er_2S_5$: $a = 391.27(2)$, $b = 1382.91(7)$, $c = 1630.54(8)$ pm; $RbCu_3Er_2S_5$: $a = 392.83(3)$, $b = 1389.7(1)$, $c = 1634.8(1)$ pm; $CsCu_3Er_2S_5$: $a = 394.82(3)$, $b = 1410.90(13)$, $c = 1667.17(19)$ pm). Concerning the surroundings of the Er^{3+} cations with S^{2-} anions, $[ErS_6]^{9-}$ octahedra are built in $TlCu_3Er_2S_5$ as well as in $Tl_2Cu_5Er_3S_8$, which result in linear ${}^1_\infty\{[Er_2S_{10}]^{14-}\}$ chains for both cases. Within the crystal structure of $TlCu_3Er_2S_5$, an anionic slab is finally formed just by connecting these chains. $Tl_2Cu_5Er_3S_8$ shows an additional kind of chains, ${}^1_\infty\{[ErS^t_{2/1}S^e_{4/2}]^{5-}\}$, where the $[ErS_6]^{9-}$ octahedra share further edges. The Er^{3+}–S^{2-} distances and angles are in slightly more narrow ranges in $TlCu_3Er_2S_5$ ($d(Er^{3+}$–$S^{2-}) = 264-276$ pm, $\angle$(S–Er–S) = 86 – 94°) than in $Tl_2Cu_5Er_3S_8$ ($d(Er^{3+}$–

S^{2-}) = 262 – 273 pm, ∠(S–Er–S) = 85 – 95°). Concerning the Cu^+ cations, there is a correspondence in that in both structures Cu^+-centered $(S^{2-})_4$ tetrahedra appear, which form $^1_\infty\{[CuS^t_{2/1}S^v_{2/2}]^{5-}\}$ chains by vertex-connection and also $^1_\infty\{[CuS^e_{2/2}S^v_{2/2}]^{3-}\}$ chains of edge- and vertex-connected $[CuS_4]^{7-}$ entities. For $TlCu_3Er_2S_5$, these two features end up in $^2_\infty\{[Cu_3S_5]^{7-}\}$ layers by sulfide fusion. Cu^+ cations situated in sulfur triangles that share vertices resulting in $^1_\infty\{[CuS^t_{1/1}S^v_{2/2}]^{3-}\}$ chains are present only in $Tl_2Cu_5Er_3S_8$. Similar bond lengths and angles within all $[CuS_4]^{7-}$ tetrahedra can be observed in both crystal structures ($TlCu_3Er_2S_5$: $d(Cu^+–S^{2-})$ = 233 – 258 pm, ∠(S–Cu–S) = 105 – 124°; $Tl_2Cu_5Er_3S_8$: $d(Cu^+–S^{2-})$ = 234 – 254 pm, ∠(S–Cu–S) = 105 – 122°). In both compounds two different types of chains of $[CuS_4]^{7-}$ tetrahedra are present simultaneously. In comparison, the $(Cu3)^+–S^{2-}$ bond lengths, which show up within the $[(Cu3)S_3]^{5-}$ triangles only in the crystal structure of $Tl_2Cu_5Er_3S_8$, are somewhat shorter ($d((Cu3)^+–S^{2-})$ = 224 – 232 pm). A combination of all these chains results in corrugated anionic slabs $^2_\infty\{[Cu_3S_5]^{7-}\}$ in $TlCu_3Er_2S_5$, and $^2_\infty\{[Cu_5S_8]^{11-}\}$ in $Tl_2Cu_5Er_3S_8$. Copper- and erbium-bearing anionic sulfide layers are alternatingly stacked in each case to give three-dimensional frameworks $^3_\infty\{[Cu_3Er_2S_5]^-\}$ for $TlCu_3Er_2S_5$ and $^3_\infty\{[Cu_5Er_3S_8]^{2-}\}$ for $Tl_2Cu_5Er_3S_8$. In both structures, these frameworks contain tunnel-like caverns, which are occupied by Tl^+ cations in a similar way. All Tl^+ cations are eightfold coordinated by S^{2-} anions in the shape of bicapped trigonal prisms that are face-connected forming $^1_\infty\{[TlS^t_{2/1}S^f_{6/2}]^{9-}\}$ chains. The bond lengths within these $[TlS_8]^{15-}$ prisms show a wider range in $Tl_2Cu_5Er_3S_8$ ($d(Tl^+–S^{2-})$ = 305 – 372 pm) as compared to $TlCu_3Er_2S_5$ ($d(Tl^+–S^{2-})$ = 324 – 347 pm). While these chains remain separated in $TlCu_3Er_2S_5$, two of them are connected in $Tl_2Cu_5Er_3S_8$, but leave a small gap in between, where the chain of vertex-sharing $[(Cu3)S_3]^{5-}$ triangles is embedded. This arrangement provides a very close proximity between the cations $(Tl1)^+$ and $(Cu3)^+$ with only 291 pm as separation, which is even smaller than the shortest $Tl^+–S^{2-}$ bond length with a distance of 305 pm. For comparison, the shortest $Tl^+\cdots Cu^+$ contact is 359 pm and shortest $Tl^+–S^{2-}$ distance is 324 pm in $TlCu_3Er_2S_5$. Furthermore, the black color of $Tl_2Cu_5Er_3S_8$ may indicate attractive $Tl^+\cdots Cu^+$ interactions *via* itinerant electrons stemming from the Tl^+ lone pairs, which are virtually not present in the orange $TlCu_3Er_2S_5$. This also indicates some 6*sp*-cation behavior with stereochemically active lone pair electrons at the Tl^+ cations within the crystal structure of $Tl_2Cu_5Er_3S_8$. It is noteworthy that upon a change from S^{2-} to Se^{2-}, the Tl^+ cations again show just a $6s^2$-like behavior, and an example for this is the crystal structure of $Tl_2Cu_5Lu_3Se_8$ [7], where no attractive $Tl^+\cdots Cu^+$ interactions can be observed, since all Cu^+ cations are tetrahedrally coordinated by Se^{2-} anions and thus avoid the Tl^+ proximity. Both compounds crystallize monoclinically in the space group *Cm* and even isopointal. Despite the substitution of Er^{3+} with the smaller Lu^{3+} cation, the lattice parameters expand due to the larger chalcogenide anion ($Tl_2Cu_5Er_3S_8$: a = 1381.69(7), b = 390.73(2), c = 1435.98(7) pm, β = 111.132(3)°; $Tl_2Cu_5Lu_3Se_8$: a = 1427.23(8), b = 404.59(2), c = 1464.37(8) pm, β = 110.521(3)°). While residing within a triangle of S^{2-} anions with a displacement of only 12 pm in $Tl_2Cu_5Er_3S_8$, the $(Cu3)^+$ cation in $Tl_2Cu_5Lu_3Se_8$ is situated markedly above a triangular plane of Se^{2-} anions (displacement: 62 pm) with an extra, but elongated bond to $(Se7)^{2-}$ ($d((Cu3)^+–S^{2-})$ = 224 – 232 pm, CN = 3, *versus* $d((Cu3)^+–Se^{2-})$ = 240 – 249 + 281 pm, CN = 3+1). Along with this expansion of the coordination number for $(Cu3)^+$ and the loss of the attractive $Tl^+\cdots Cu^+$ interactions ($d((Cu3)^+\cdots(Tl1)^+)$ = 327 pm, $d((Cu3)^+\cdots(Tl2)^+)$ = 325 pm, 2 ×), the corrugated $^2_\infty\{[Cu_5S_8]^{11-}\}$ layers in $Tl_2Cu_5Er_3S_8$ are fused to a three-dimensional framework $^3_\infty\{[Cu_5Se_8]^{11-}\}$ in $Tl_2Cu_5Lu_3Se_8$ [7].

[1] J. Yao, B. Deng, D. E. Ellis, J. A. Ibers, *J. Solid State Chem.* **2003**, *176*, 5.

[2] P. Stoll, P. Dürichen, C. Näther, W. Bensch, *Z. Anorg. Allg. Chem.* **1998**, *624*, 1807.

[3] J. Yao, J. A. Ibers, *Acta Crystallogr.* **2004**, *E60*, i118.

[4] F.-Q. Huang, J. A. Ibers, *J. Solid State Chem.* **2001**, *158*, 299.

[5] P. Lauxmann, Th. Schleid, *Z. Naturforsch.* **2001**, *56b*, 1149.

[6] M. A. Eberle, Th. Schleid, unpublished results.

[7] J.-M. Babo, Th. Schleid, T. E. Albrecht-Schmitt, *Z. Anorg. Allg. Chem.* **2012**, *638*, 2485.
[8] R. J. Havighurst, *J. Am. Chem. Soc.* **1926**, *48*, 2113.
[9] L. Karanovic, D. Poleti, T. Balić-Žunić, E. Makovicky, I. Grzetic, *J. Alloys Compd.* **2008**, *457*, 66.
[10] W. Herrendorf, H. Bärnighausen, HABITUS, Program for the Optimization of the Crystal Shape for Numerical Absorption Correction, as contained in X-SHAPE (version 1.06, Stoe & Cie GmbH, Darmstadt, Germany), Karlsruhe, Gießen (Germany) **1993**, **1996**.
[11] G. M. Sheldrick, *Acta Crystallogr.* **2008**, *A64*, 112.
[12] Th. Hahn, A. J. C. Wilson (Eds.) *International Tables for Crystallography,* Vol. C, 2nd edition, Kluwer Academic Publishers, Boston, Dordrecht, London, **1992**.
[13] R. X. Fischer, E. Tillmanns, *Acta Crystallogr.* **1988**, *C44*, 775.
[14] R. Hoppe, *Adv. Fluorine Chem.* **1970**, *6*, 387.
[15] J.-M. Babo, *Dissertation*, University of Stuttgart, Stuttgart **2010**.
[16] R. D. Shannon, *Acta Crystallogr.* **1976**, *A32*, 751.